Available online www.jsaer.com

***Journal of Scientific and Engineering Research*, 2025, 12(4):13-26**

Research Article

ISSN: 2394-2630
CODEN(USA): JSERBR

Carbon Sinks in Chengdu's Urban Buildings: A Study Considering Climate Impacts

Yuxiao Sha, Lingwei Ran, Ruiqi Zhao*

School of Materials Science and Engineering, Henan Polytechnic University, Jiaozuo 454003, China
***Corresponding author: Ruiqi Zhao (Email: zhaoruiqi@hpu.edu.cn)

Abstract: Carbon sinks in urban buildings are realized through chemical reactions between the concrete in the building and the CO_2 in the air. Accurate quantification of carbon sinks in urban buildings can help to achieve the "dual carbon" target. In this study, we developed a predictive model described with the exposed area and completion time of a building. Using the model, we investigated the carbon sinks of existing buildings within the Third Ring Road in Chengdu city over the past 50 years. Three factors including the effects of concrete strength, climatic conditions, and window-to-ground ratio we considered in constructing the model. The results show that the total amount of carbon sinks within Chengdu's Third Ring Road is 507, 457 tons, of which 72.49% comes from residual buildings. The density of carbon sinks is unevenly distributed, mainly concentrated in the middle and left parts of the area. In addition, the building carbon sinks show a high degree of time-dependence and have increased significantly over the last 30 years. This increase is mainly attributed to the increase in the number of residual buildings. This work not only visualizes the spatial distribution of the carbon sinks, but also provides practical solutions to improve the carbon sinks, thus should provide a sustainable path for urban greening and urban ecology.

Keywords: Pega, Queue Processor, Standard Agent, Apache Kafka, Background Task Management, Asynchronous Processing, Enterprise Applications, Scalability, Fault Tolerance, Stream Service

1. Introduction

With rapid industrialization, economic and demographic development, CO_2 emissions are huge and growing at an unprecedented rate. It is reported that the total carbon emissions in 2023 were 37.4 billion tons, of which 12.6 billion tons are from China [1]. The massive emission of CO_2 leads to the greenhouse effect, the immediate danger of which is an increase in atmospheric temperature. Average temperatures are reported to be 1.0 ℃ above the pre-industrial levels and rising by 0.2 ℃ per decade [2-3], accelerating polar and glacier melting, sea level rise [4], river flooding, and extinction of species [2]. To reduce CO_2 emissions, at the 75th General Debate of the United Nations General Assembly, the Chinese government pledged to implement a "dual carbon" plan to cap carbon emissions by 2030 and achieve carbon neutral by 2060 [5].

In order to achieve the "dual-carbon" target, it is important to accurately assess CO_2 emissions and understand where the CO_2 is going. Concrete and concrete-related cementitious materials are widely used in modern construction [6]. Global concrete production is reported to be close to 12 billion tons per year [7]. The production of 1 ton of cement will produce 0.369 tons of CO_2 [8]. In fact, the cement and cement-related cementitious materials in concrete can absorb CO_2 through spontaneous reactions with atmospheric CO_2 [9-10]. This spontaneous process is known as a carbon sink [11]. The construction accounts for 40% of total carbon emissions and is therefore considered a major contributor to carbon emissions [12]. To assess the building carbon sink, Zhang [13] reported that the carbon sequestration rate of a three-story reinforced concrete building is about 36.9%, which suggests that the building carbon sink cannot be ignored when calculating the net carbon emissions. Xi et al. [14] reported that the cement absorbs 43% of the CO_2 released during the cement production over its lifecycle. Using a comprehensive analytical model, Huang et al. [15], reported that the cumulative amount of CO_2 absorbed by cement globally during the period 1930-2021 was 22.9 Gt, which accounted for 55.1% of the total CO_2 released from cement production during the same period. The above studies show that buildings play an active role in sequestering CO_2.

In order to assess the contribution of the building carbon sink, it is necessary to quantify the building carbon sink. Andersson et al. [16] developed a theoretical model to calculate the CO_2 sequestration of existing concrete structures in Sweden and reported a CO_2 uptake of about 300, 000 tons in 2011, which accounted for 17% of the CO_2 emissions from cement production in the same period. Li [17] combined a single building carbon sink calculation model and a regional building carbon sink calculation model to explore the main factors affecting the carbonization of concrete. Yang et al. [18] conducted a comparative analysis of office buildings and residences in South Korean based on Fick's second law. Using the model, they reported that carbon sinks accounted for 15.5-17% of the CO_2 emissions generated during the production of concrete in buildings over the 100-year life cycle of the building. However, the study covered a small area and the results obtained cannot be used to study the carbon sinks of all buildings in a city. Li [19] developed a city-scale carbon sink model for urban buildings using the concrete carbonation rate coefficients reported by Xi et al. [14]and investigated the carbon sink of urban buildings within the Third Ring Road in Shenyang. The carbonization rate coefficients were only recalculated using coefficients from different regions, which may lead to higher predictions of natural carbon sinks in soil and above-ground vegetation in the same area. In our recent work, we developed a simple model to study the carbon sinks of urban buildings in the Third Ring Road in Zhengzhou city over the past 50 years [20]. The model was described in terms of the exposed area of the buildings and the completion time of construction. However, the window-to-ground ratio is not taken into account when calculating the exposed area. How does the window-to-ground ratio affect the carbon sink of a building? In addition, diffusion of CO_2 through concrete can also affect CO_2 uptake in buildings. The diffusion process has been reported to be governed by a number of factors, including CO_2 concentration, ambient temperature and relative humidity [21]. These factors are closely related to climatic conditions, which are largely dependent on the geographical location of the city. How does geographical location affect the carbon sinks?

In order to answer these questions, we conducted a systematic study of building carbon sinks in the Third Ring Road area of Chengdu. Firstly, the characteristic parameters of the prediction model were determined on the basis of corrections for climatic conditions and window-to-ground ratio. Second, the validity of the developed model was further verified using 26,821 buildings in 400point blocks in the target area. Third, the carbon sinks of all urban buildings in the study area were calculated using the developed model. Then, the density distribution of the carbon sinks, the carbon sinks at different time, and the relationship between the carbon sinks and the number of buildings were discussed. Based on these data, procedures and other work to increase carbon sinks in urban building are proposed.

2. Study region, data processing and models

Study region

Sichuan is located almost in the center of China (Fig. 1a). Chengdu, the capital of Sichuan province, is located between 102°54'-104°53'E and 30°05'-31°26'N (Fig. 1b). It is reported that by the end of 2022, Chengdu will cover an area of 14,335 km2 and have a resident population of 21.268 million [22]. It is interesting to study the carbon sinks of urban buildings in this city. Here, we will focus on the carbon sinks of urban buildings in the Third Ring Road of Chengdu. The area covers 192 km2 and includes six districts: Jinniu, Qingyang, Wuhou, Jinjiang, Longquanyi and Chenghua (Fig. 1c).

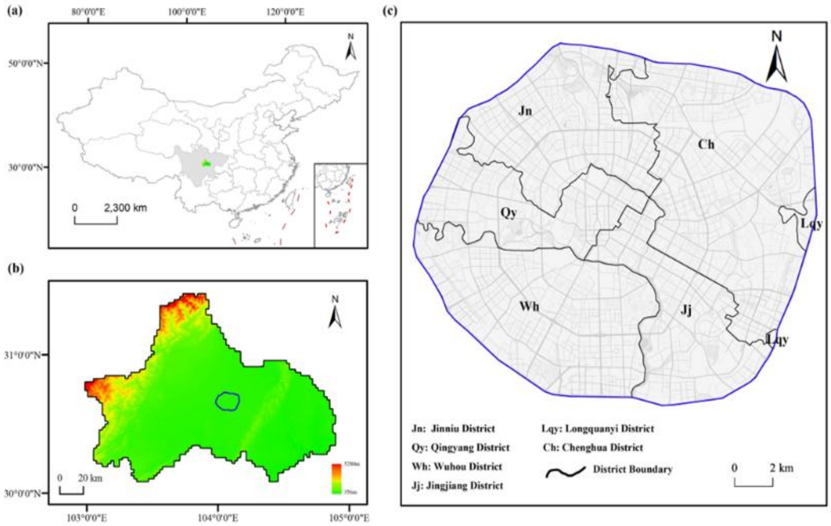

Figure 1: (a) Schematic map of China. The grey and colored areas represent Sichuan Province and Chengdu city, respectively. (b) Schematic map of Chengdu. The color ranging from green to red represents the topographic elevation changes in Chengdu, and the area enclosed by the blue line represents the area of this study. (c) The area of the Third Ring Road of Chengdu and its constituent districts.

Data processing

Sampling and field survey

The basic data used in this work are vector data downloaded from BIGEMAP and satellite image data (with a resolution of 0.5 m). The remote sensing influence is used to derive the shadow lengths of the buildings, extract the heights of the buildings, and finally obtain the 3D spatial information of the buildings [23]. In this study, 400 point blocks were randomly arranged in the study area according to different building characteristics such as building type, exposed area and building height. In order to ensure the integrity of the buildings, the shapes of these point blocks were modified according to the road network boundaries (see Fig. 2a). Based on the functional characteristics of the buildings, the buildings were categorized into five types, including residential buildings (RB), industrial buildings (IB), commercial buildings (CB), public service buildings (PB) and other buildings (OB). Fig. 2b shows the distribution of these building within the within the closed area in Fig. 2a. There are 26,821 buildings in the 400 point blocks.

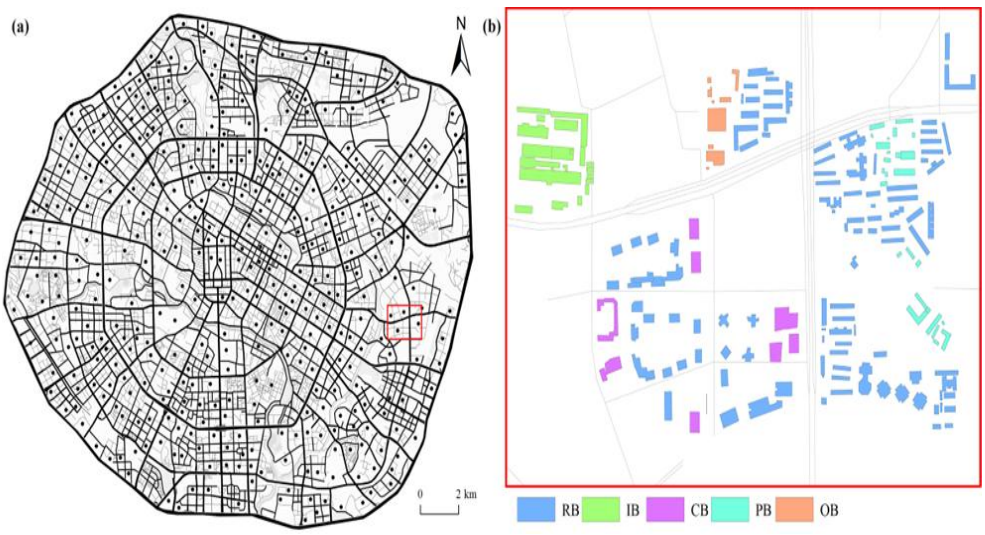

Figure 2: (a) Sampling points in the area of the Third Ring Road of Chengdu. (b) Distribution of different types of buildings (RB, IB, CB, PB and OB) in the red rectangular area.

Parameters used to characterize different types of buildings

There are many parameters that can be used to characterize different types of buildings. Common parameters are: building type, number of buildings of each type, average data of exposure time (t), number of floors of the building (F), height of the building (H), perimeter of the building base (p), area of the building base (Ab1), capacity of the building (Cb), area of the building (Ab2), and exposed area of the building (Ae). The details of these parameters are summarized in Table 1.

Table 1: Building type, number of buildings, and average data used to characterize the building, including exposure time (t), number of building floors (F), building height (H), perimeter of the building base (p), area of the building base (A_{b1}), capacity of the building (C_b), area of the building (A_{b2}) and exposed area of the building (A_e).

Type	Number	Average data							
		t (a)	F	H(m)	P (m)	A_{b1} (m^2)	C_b (m^3)	A_{b2}^* (m^2)	A_e (m^2)
RB	18,197	22.99	9.14	32.00	149.15	873.22	32,145.58	9,184.45	27,999.28
IB	756	32.77	2.89	14.51	127.69	1,019.79	16,171.98	3,253.84	10,937.57
CB	3,452	20.38	7.25	35.19	161.58	1,405.00	57,408.49	11,817.85	35,906.58
PB	4,219	46.78	5.69	21.16	143.69	977.99	21,884.60	5,871.29	18,165.13
OB	197	16.81	2.73	8.19	107.54	641.43	5,984.54	1,994.85	6,104.90

* A_{b2} is calculated from the formula $A_{b2} = A_{b1} \cdot F$

Buildings with different heights and types require different compressive strengths of concrete, which can be determined according to the Construction Engineering Calculation Manual [24]. The cement content of concrete of different strengths can be determined according to the Design Procedure for Proportions of Ordinary Concrete [25]. The details of building type, sub-divisions, concrete grade and cement content are summarized in Table 2.

Table 2: Building type, sub-division, concrete grade, and mass of cement per cubic meter of concrete

Type	Sub-divisions	Concrete grade	Cement mass(kg/m^3)
RB	Low-rise	C30	400
	Mid-rise	C35	402
	High-rise	C40	419
IB	Low-rise	C30	400
	High-rise	C35	402
CB	Stores	C30	400
	Office building	C40	419
	Shopping center	C45	462
PB	Executive office	C30	400
	Medical service	C35	402
	Educational/research institutions	C40	419
OB	Low-rise	C30	400
	High-rise	C35	402

Another factor that should not be overlooked in calculating the carbon sink of a building is the windows, which have a large exposed area ratio. Typically, the window-to-ground ratio, i.e., the ratio of window area to the floor area of a room, is used to describe the impact of windows on carbon sinks in different types of buildings. The window-to-ground ratios for the RB, IB, and the other three types (CB, PB, and OB) of buildings are 0.17 [26], 0.13 [27]and 0.20 [28-29], respectively.

Parameters used to characterize different types of buildings

There are many factors that affect the carbonation rate of concrete, such as CO2 concentration, relative humidity and air temperature. It increases with increasing temperature and CO2 concentration, and increases then decreases with increasing relative humidity. In order to obtain a good carbon sink model, the carbonation rate must be determined according to the climatic characteristics of the target area. Chengdu belongs to the subtropical humid monsoon climate zone, with sufficient heat, abundant rainfall, four distinct seasons, and simultaneous rain and heat. According to statistics [30], from 1998 to 2022, the annual average temperature, relative humidity and rainfall are 16.7 ℃, 78% and 915.6 mm, respectively. The average temperature, relative humidity and rainfall of each year from 1998 to 2022 are shown in Fig. 3.

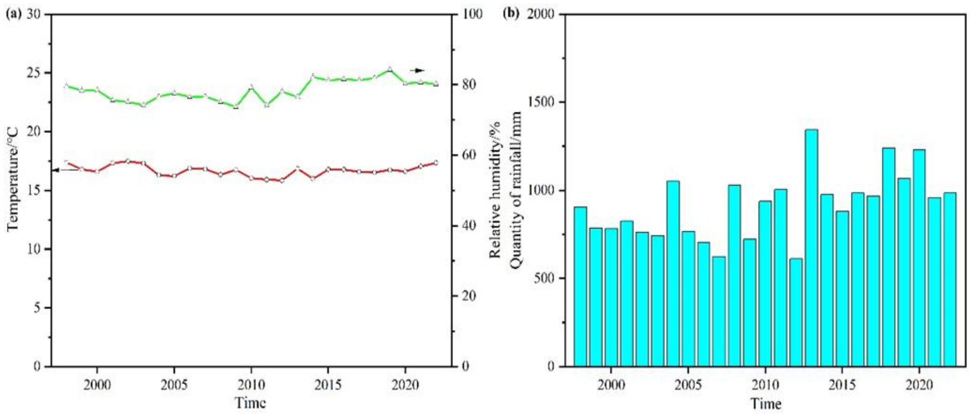

Figure 3: (a) Mean annual air temperature and relative humidity in Chengdu from 1998 to 2022; (b) Annual rainfall in Chengdu from 1998 to 2022.

The carbonation rate coefficient of concrete can be calculated by the following equation [31]:

$$k = k_{nw}(T/10)^{0.713}(RH^2 - 1.98RH^2 + 1.896)\sqrt{\frac{C_0}{0.03}}\left(\frac{15.806}{f_{cu}} + 0.215\right). \quad (1)$$

where k is the carbonation rate coefficient, mm/a0.42; knw is the indoor and outdoor concrete carbonation factor, here indoor and outdoor respectively take 1.87 and 1.0; T is the ambient temperature, ℃; RH is the ambient relative humidity, %; C0 is the ambient CO2 volume concentration, %; fcu is the standard value of the compressive strength of the cubic concrete, MPa. Combined with the Chengdu's climatic and environmental conditions, the carbonation rate coefficients can be derived (see Table 3 for details). The average value of k is used to calculate the carbonation depth of concrete.

Table 3: Carbonation rate coefficients of concrete with different strength for different building types.

Environmental		Carbonation rate coefficient, *k* (mm/a$^{0.42}$)											
		≤15 MPa			16-20 MPa			23-35 MPa			＞35 MPa		
		Max	Min	Avg	Max	Min	Avg	Max	Min	Avg	Max	Min	Avg
Indoor	RB	8.32	4.60	6.30	5.57	3.64	4.50	4.18	2.42	3.13	3.09	2.05	2.51
	IB	7.78	2.80	4.95	5.21	2.22	3.54	3.91	1.47	2.46	2.89	1.25	1.97
	CB	8.71	1.64	5.98	5.83	1.30	4.27	4.37	0.86	2.97	3.23	0.73	2.38
	PB	8.58	1.34	5.45	5.75	1.06	3.89	4.31	0.70	2.70	3.18	0.60	2.17
	OB	10.21	3.74	6.70	6.84	2.96	4.78	5.13	1.97	3.32	3.79	1.48	2.67
outdoor		4.34	0.51	2.37	2.91	0.40	1.69	2.18	0.27	1.18	1.61	0.24	0.95

Carbon sinks in individual buildings

Carbon sinks in buildings mainly come from the carbonation reaction between the chemical components in concrete and CO_2 in the air. Carbon sinks in buildings mainly refer to the amount of carbon absorbed by the carbonation reaction [32]. According to the law of conservation of mass, the amount of carbon sequestered in concrete can be calculated from the mass of cement involved in the carbonation reaction as follows [33]:

$$MM_c = \emptyset_c \cdot C_p \cdot W_c \tag{2}$$

where M_c is the amount of carbon sequestered in the concrete of a single building, kg; Ø_c is the degree of carbonation, and in this study it is assumed that the cement minerals are fully carbonated, i.e., Ø_c=1.0; C_p is the carbon sequestration potential, i.e., the ratio of carbon dioxide absorbed by per unit mass of cement to the total mass of cement; and W_c is the mass of cement involved in the reaction, kg, and it is related to the volume of concrete involved in the reaction in the building and the cement content per unit volume of concrete.

The carbon sequestration potential C_{pis} calculated as follows:

$$C_p = C_{clinker} \cdot f_{CaO} \cdot \gamma \cdot M_\gamma \tag{3}$$

where $C_{clinker}$ is the proportion of clinker in cement, ranging from 75% to 97% [34]; f_CaO is the proportion of CaO in cement clinker, which is generally taken as 65% [35-36]; γ is the proportion of CaO in concrete that is fully carbonated to $CaCO_3$, with an average value of 0.8; and M_γ is the ratio of C to CaO with a value of 0.214.

The formula for calculation of W_c is:

$$W_c = V_c \cdot m \tag{4}$$

where V_c is the total volume of carbonated concrete, m3; m is the mass of cement per unit volume of concrete, kg/m^3. Details of the mass of cement used in different types of buildings are summarized in Table 2.

Due to the different carbonation rates of concrete in different environments, the carbonation of cement can be divided into two parts: indoor and outdoor. The calculation is as follows:

$$V_c = d_i \cdot A_i + d_o \cdot A_o \tag{5}$$

where d_i and d_o represent the depth (m) of carbonation of indoor and outdoor concrete, respectively; A_i and A_o represent the exposed area (m^2) of indoor and outdoor concrete, respectively.

The carbonation process of concrete is very complicated. Many scholars at home and abroad have studied the carbonation depth and proposed different prediction models. Combining the research results of Zhang [31]and Fick's second law, the carbonation depth d can be described as:

$$d_i = k_i \cdot t^{0.42} \tag{6}$$

$$d_o = k_o \cdot t^{0.42} \tag{7}$$

where t is the exposure time of the building, which is equal to the completion time of the building.

Modelling of carbon sinks in urban buildings

The amount of CO_2 absorbed by the 26,821buildings located in 400 point blocks can be calculated based on equations 1-7 above. With these data, it is possible to build a model for predicting the carbon sinks of all buildings in the target area. In order to a suitable model, 8 separate parameters characterizing the buildings were considered in the prediction model. In order to select the most appropriate parameter, a Pearson correlation analysis was carried out. The closer the Pearson correlation coefficient is to 1, the better the correlation is. The Pearson correlation coefficients between building characteristics and carbon sinks are presented in Table 4. Table 4, it can be seen that the exposed area Ae has the best correlation with the carbon sink of the buildings. Therefore, Ae will be used as a key parameter in the prediction model. According to Zhang's study [31] and Fick's law [37], the exposure time, t0.42 is another parameter to be considered for predicting carbon sinks in buildings.

Table 4: Pearson correlation coefficients (P) between carbon sinks and eight independent parameters describing characteristics of different types of buildings. The parameters include concrete strength (Cs), the number of building floors (F), building height (H), building base perimeter (p), building base area (Ab1), building capacity (Cb), building area (Ab2) and exposed surface area (Ae).

P / Type	P_{C_s}	P_F	P_H	P_p	$P_{A_{b1}}$	P_{C_b}	$P_{A_{b2}}$	P_{A_e}
RB	0.442	0.519	0.519	0.729	0.845	0.937	0.938	0.952
IB	0.377	0.347	0.347	0.815	0.795	0.947	0.950	0.962
CB	0.219	0.518	0.529	0.644	0.678	0.952	0.951	0.961
PB	0.185	0.434	0.412	0.612	0.620	0.970	0.974	0.991
OB	0.293	0.282	0.298	0.809	0.891	0.940	0.949	0.956

In this study, three carbon sink prediction models were developed, namely, a stepwise regression model, a linear regression model and a power function regression model. The reliability of each model was assessed by the goodness-of-fit R^2. The closer the R^2 is to 1, the more reliable the model is. The models used for predicting carbon sinks in different types of buildings and their corresponding goodness-of-fit R^2 are summarized in Table 5. It can be seen that all three types of models show good reliability in predicting carbon sinks in buildings, with the powder function regression model being the most reliable. Therefore, the powder function regression model (highlighted in bold in Table 5) will be used to predict the carbon sinks of all buildings.

Table 5: Type of prediction model, building type, model equations and goodness-of-fit, R^2. Model equations with the largest R^2 are shown in bold.

Type of regression model	Building type	Model equations	R^2
Stepwise regression	RB	$Y = 0.267A_e + 2696.902t^{0.42} - 8250.683$	0.929
	IB	$Y = 0.303A_e + 866.220t^{0.42} - 3554.868$	0.945
	CB	$Y = 0.276A_e + 3652.542t^{0.42} - 11709.332$	0.939
	PB	$Y = 0.262A_e + 1752.255t^{0.42} - 6258.087$	0.629
	OB	$Y = 0.279A_e + 705.112t^{0.42} - 2182.315$	0.925
Linear regression	RB	$Y = (0.094A_e + 113.825)t^{0.42}$	0.993
	IB	$Y = (0.076A_e - 25.652)t^{0.42}$	0.997
	CB	$Y = (0.093A_e - 36.230)t^{0.42}$	0.995
	PB	$Y = (0.085A_e - 103.144)t^{0.42}$	0.991
	OB	$Y = (0.093A_e + 16.466)t^{0.42}$	0.995
Power function regression	RB	$\boldsymbol{Y = (0.092A_e^{1.008})t^{0.42}}$	**0.997**
	IB	$\boldsymbol{Y = (0.053A_e^{1.032})t^{0.42}}$	**0.999**
	CB	$\boldsymbol{Y = (0.077A_e^{1.017})t^{0.42}}$	**0.998**
	PB	$\boldsymbol{Y = (0.056A_e^{1.033})t^{0.42}}$	**0.995**
	OB	$\boldsymbol{Y = (0.081A_e^{1.019})t^{0.42}}$	**0.996**

3. Results and discussion

Reliability and generalizability of the prediction model

The prediction model is described by the exposed area of the buildings and the completion time. In order to verify the reliability of the developed model, the carbon sinks of 26,821 buildings in 400 point blocks were calculated. The comparison of the calculated values with the predicted values is shown in Fig. 4. From Fig. 4, it can be seen that the R2 of goodness-of-fit for all buildings is between [0.995, 0.998]. The high R2 indicates that the model we developed has good reliability. In addition, the model takes into account the window-to-ground ratio when calculating the exposed area of the buildings. This correction makes the exposed area more suitable to characterize real buildings, thus providing more reasonable results for predicting carbon sinks in urban buildings.

It is worth noting that the model has only two parameters, namely the exposed area of the building and the time of completion. The former parameter can be easily obtained by interpreting high-resolution remote sensing images. The latter parameter can be obtained from commonly used maps such as Gaode. These parameters are simple and easy to obtain, which can effectively ensure that the model has good generalizability.

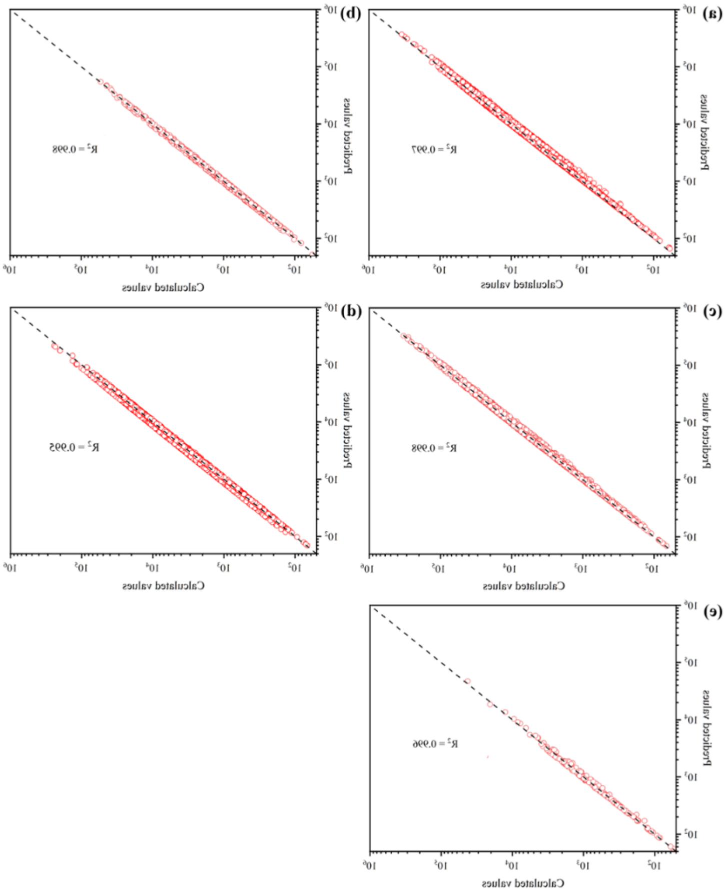

Figure 4: Comparison of predicted and calculated carbon sinks for different types of buildings: (a) RB, (b) IB, (c) CB, (d) PB, and (e) OB. The dashed line y = x is also presented for eye guidance.

Carbon sinks and their spatial distribution in the study area

The developed model was used to predict the carbon sinks of all buildings within the Third Ring Road in Chengdu. There are 59,207 buildings in the target area, generating a total of 507,457 tons of carbon sinks between 1973 and 2023. The contribution of each building type is shown in Fig. 5a. It can be seen clearly from the figure that RB contributes the largest amount of carbon sinks, followed by CB, and then PB, IB, and OB. In order to understand the potential of the buildings' contribution, the carbon sink density, dB, was introduced to determine the carbon sink capacity of each building type. Unlike the carbon sinks of buildings, the buildings PB has the largest potential of carbon sinks, followed by RB, IB, CB and OB. The number, area, carbon sink, carbon sink ratio and carbon sink density of each type of buildings are summarized in Table 6.

Table 6: Building type, number, area, carbon sink, carbon sink ratio and carbon sink density of each type of buildings, dB.

Type	Number	Area* (hm^2)	Carbon sink (t)	Ratio	d_B** (t/hm^2)
RB	41,040	36,475	367,832	72.49%	10.08
IB	1,443	503	4,960	0.98%	9.87
CB	6,523	8,387	78,219	15.41%	9.33
PB	8,882	4,719	52,448	10.34%	11.12
OB	1,319	512	3,998	0.79%	7.81

The spatial distribution of carbon sinks is another important data to understand the specific contribution of each building type. To obtain this data, the distribution of different types of buildings is first determined according to the land use plan of Chengdu city (Fig. 5b) Combining the land use planning and urban building vector data, the spatial distribution of carbon sinks can be derived (see Fig. 5c). From Fig. 5c, it can be seen that the distribution of carbon sinks is not uniform throughout the study area. In general, the areas with larger contributions of carbon sinks are consistent with the areas where commercial buildings are located. In order to further show the distribution of carbon sinks within the study area, a regional carbon sink density dA was introduced, which is the carbon sink divided by the area of the region. The study area was divided into equal-sized blocks of fishing nets. The regional carbon sink density for the entire study area is shown in Fig. 5d. It can be seen that the distribution of the regional carbon sink density is uneven. The areas with higher regional carbon sink density are mainly located in the center and left part of the study area. This distribution is mainly related to the densely built-up residential area. On the contrary, the right side of the area with lower regional carbon sink density is dominated by other buildings such as transport stations, which are less densely built up.

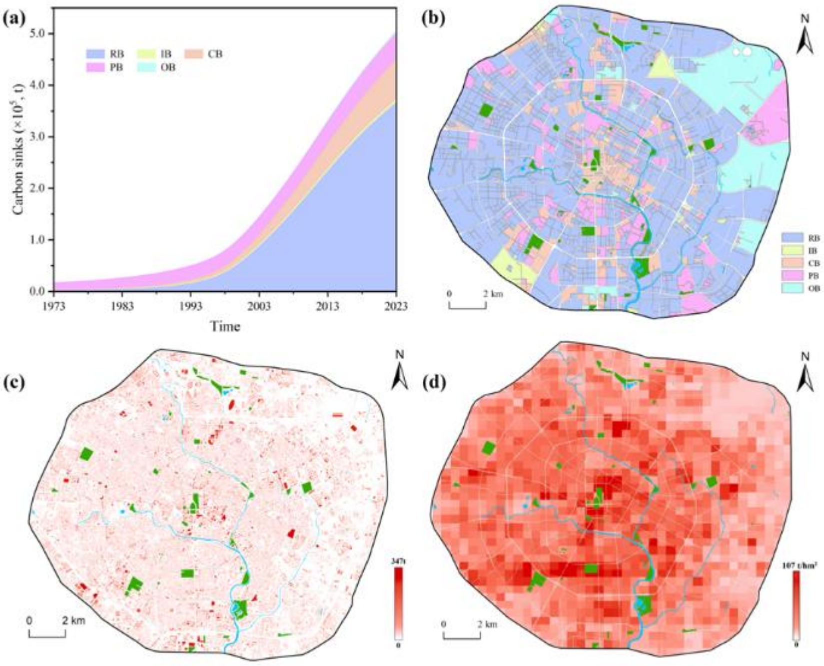

Figure 5: (a) Carbon sinks of different types of buildings. (b) Distribution of land types in the area of the Third Ring Road of Chengdu. (c) Distribution of carbon sinks. Changes in the depth of red color represent changes in carbon sinks. (d) Distribution of the regional carbon sink density. Green and blue colors in (b-d) represent parks and rivers respectively. Carbon sinks in these areas are not considered.

Factors affecting carbon sinks

The carbon sinks in Fig. 5a show definitely increase over time. However, both the amount and increasing trend are quite different for different types of building. There are many factors that influence the carbon sinks of urban buildings. In order to clarify the specific role of these factors, in the following part, we will discuss the influence of different factors in the following sections.

Number of buildings

The carbon sinks contributed by different types of buildings show very different variations over time (see Fig. 5a). This feature may be related to changes in the number of buildings over time. In order to reveal the effect of the number of buildings on carbon sinks, the number of existing buildings and carbon sinks were conducted every ten years. The results are shown in Fig. 6a and b, respectively. From Fig. 6a, it can be seen that the number of RB-type buildings increases significantly, especially from 1993 to 2023. As for PB-type buildings, their number has increased almost steadily over the past 50 years. As for IB- and OB-type buildings, the increase in their numbers is relatively small. Combined with Fig. 6b, it can be seen that the increasing trend of carbon sinks is consistent with the increasing trend of the number of buildings. Therefore, it can be assumed that the sharp increase in carbon sinks of RB and CB buildings (from 2003 to 2023) is due to the increase in the number of buildings.

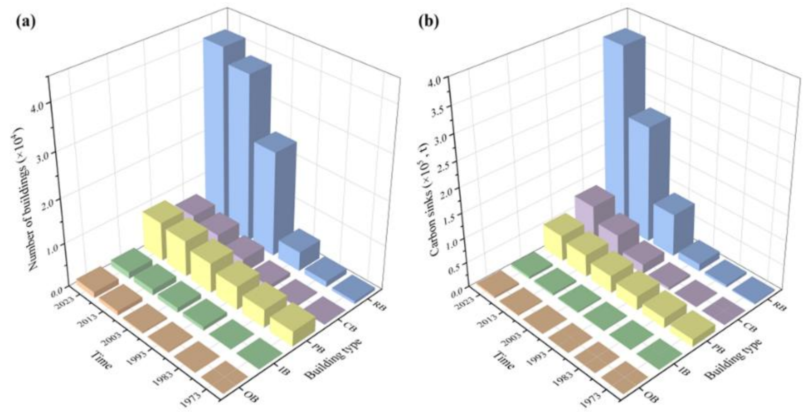

Figure 6: (a) Number of existing buildings counted per decade. (b) Carbon sinks in urban buildings per decade.

Climatic factors

The geographical location of a city also affects the carbon sink of a building, as different geographical locations lead to significant differences in factors such as CO2 concentration, relative humidity and temperature. In order to assess the impact of climatic factors, we also calculated the carbon sinks of different types of building using Xi's carbonization rate coefficients (see Table 7 for detailed data) [38]. The comparison between predicted and calculated carbon sinks is shown in Fig. 7. It can be seen that the values from this work are densely distributed around the y = x line, whereas the data calculated using Xi's carbonization rate coefficients are more dispersed in distribution, especially in case with RB and PB buildings. For better comparison, the goodness-of-fit R2 between the predicted and calculated carbon sinks is shown in Fig. 8. As can be seen in Fig. 8, the R2 values of this work are consistently higher than those obtained using the Xi carbonization rate coefficients, which suggests that the calculated values of this work match the predicted values better than those calculated using the Xi carbonization rate coefficients. It should be noted that there is a significant difference in R2 of RB- and PB-type buildings (see Fig. 8). The reason for this large difference may be related to the higher density of people in these two types of buildings, which leads to higher ambient temperatures and promotes the carbonization of the concrete. However, for the carbonization rate coefficients derived by Xi, they did not take into account the effect of environmental factors. These results suggest that climatic factors cannot be ignored in the study of carbon sinks in urban buildings.

Table 7 Carbonation rate coefficients reported by Xi et. al for different strengths of concrete in different types of buildings.

Environmental		Carbonation rate coefficient, k (mm/a$^{0.42}$)											
		≤15 MPa			16-20 MPa			23-35 MPa			＞35 MPa		
		Max	**Min**	**Avg**	**Max**	**Min**	**Avg**	**Max**	**Min**	**Avg**	**Max**	**Min**	**Avg**
Indoor	RB	5.18	2.17	4.19	4.18	2.71	3.36	5.25	1.50	2.88	2.92	0.77	1.56
	IB	13.47	3.37	6.02	6.02	3.49	5.16	4.91	3.32	4.16	3.41	1.98	2.69
	CB	7.13	4.70	5.83	5.50	4.56	5.06	5.90	2.37	4.12	2.97	1.87	2.33
	PB	6.15	4.02	4.84	5.44	3.23	3.82	5.95	2.43	3.39	2.50	1.16	1.68
	OB	6.11	4.51	5.24	5.89	1.41	4.39	3.94	2.74	3.43	1.94	1.48	1.71
outdoor		4.80	2.00	3.34	4.50	1.10	2.59	3.90	0.30	2.18	1.60	0.24	0.98

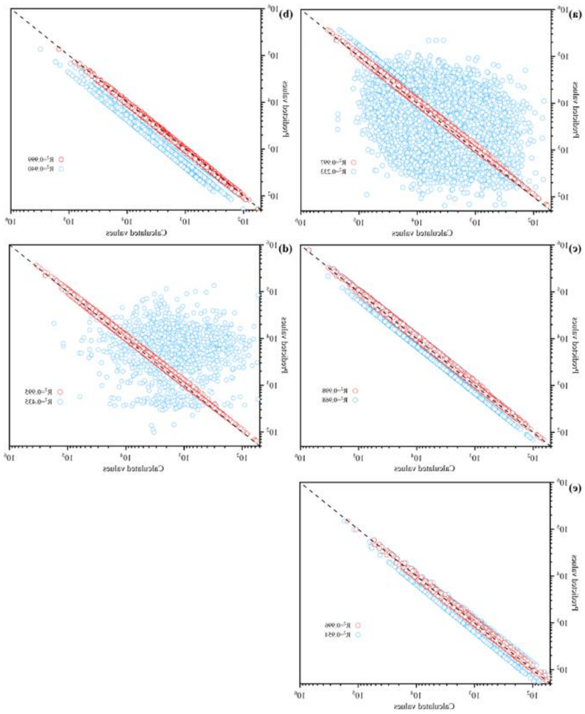

Figure 7: Comparison of predicted and calculated carbon sinks for different building types: (a) RB, (b) IB, (c) CB, (d) PB, and (e) OB. Calculated carbon sinks in the red data are based on the carbonation rate coefficients from this work, and those in the blue data are based on the carbonation rate coefficients from Xi et. al.

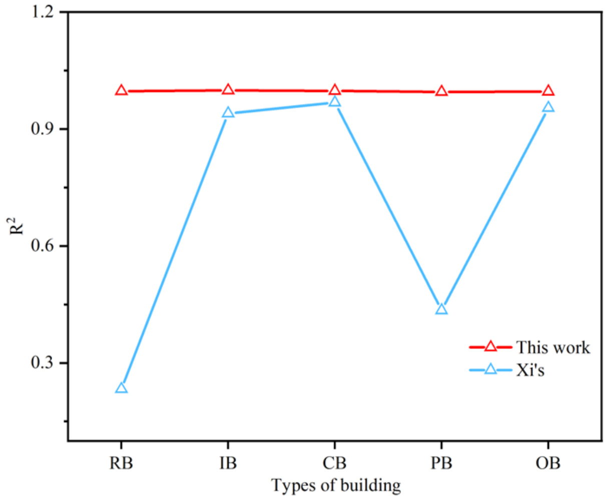

Figure 8: Comparison of R^2 from this work with R^2 calculated using Xi's carbonization rate coefficients. The carbonization rate coefficients in this work take into account the climatic factor, whereas the carbonization rate coefficients of Xi do not take into account the climatic factor.

Procedures of improving carbon sink capacity in urban buildings

The distribution of urban land use and carbon sinks of different types of buildings shows that high carbon sinks are concentrated in residential and the central business districts, and that the carbon sink capacity of buildings can be extended by prolonging the use of these buildings. Buildings are demolished when they exceed their service life, resulting in a significant increase in exposed concrete area. Recycling waste concrete as aggregate is a "kill two birds with one stone" solution that reduces costs and increases carbon sink of the building. Recycling of waste concrete has been reported to have a huge carbon sequestration potential of 5-10 billion tons, generating calcium carbonate that can sequester CO_2 in the conventional environment for a up to 1 million years [39].

Possible work in the future

Although the model shows good reliability, user-friendliness and versatility, there are still some issues that need to be considered in order to develop a more rational model in the near future. For example, the role of some building components (e.g. columns, beams and wall panels between different rooms) was not taken into account. As for the internal factors affecting the diffusion of CO_2 in concrete, only the compressive strength class of concrete was considered. However, factors such as water-cement ratio, varieties and particle size of aggregate, and admixtures can also affect diffusion of CO_2 [40-41]. In addition, some buildings are usually covered with coatings, and differences in the type of coating also have different effects on the carbonization of concrete [42-43]. Xi reported that plastering mortar reacts with CO_2 and exhibits the potential for carbon sinks [14].

4. Conclusion

Based on the statistics of climatic conditions and characteristics of buildings, a prediction model described with building exposed area and exposure time was developed. The carbon sinks of existing buildings in the Third Ring Road area of Chengdu city were studied using the model, and the results showed that:

1) The carbon sink capacities of buildings are different, and the carbon sink contributions of different types of buildings are in the order of “Residual buildings > Commercial buildings > Public buildings > Industrial buildings > Other buildings”, and the carbon sink capacities are in the order of “Public buildings > Residual buildings > Industrial buildings > Commercial buildings > Other buildings”;
2) The total amount of carbon sinks is 507,457 ton, and the density of carbon sinks is unevenly distributed, mainly concentrated in the central and the left half of the region;
3) The carbon sink of urban buildings has increased significantly over time in the last 50 years, especially in the last 30 years, the carbon sink of RB-type buildings has increased more. This feature is caused by the remarkable increase in the number of RB buildings;
4) Climate affects the carbonation rate coefficient and cannot be ignored in the study of carbon sinks of urban buildings.

Acknowledgment

This work was supported by the Innovation Scientists and Technicians Troop Construction Projects of Henan Province (no. CXTD2017089).

References

[1]. IEA, CO2 Emissions in 2023, 2024.

[2]. S. Fawzy, A.I. Osman, J. Doran, D.W. Rooney, Strategies for mitigation of climate change: a review, Environ Chem Lett 18(6) (2020) 2069-2094.

[3]. J. Launer, Climate change: Beyond denial and grief, Postgrad Med J 1119(95) (2019) 59-60.

[4]. F.N. Walls, D.J. McGarvey, A systems-level model of direct and indirect links between environmental health, socioeconomic factors, and human mortality, Sci Total Environ 874 (2023) 162486.

[5]. X. Lyu, K. Yang, J. Fang, Utilization of resources in abandoned coal mines for carbon neutrality, Sci Total Environ 822 (2022) 153646.

[6]. H. Krour, N. Tazi, R. Trauchessec, A. Ben Fraj, A. Lecomte, R. Idir, L. Barnes-Davin, B. Bolze, A. Delhay, Industrial-scale valorization of fine recycled aggregates in cement raw meal: Towards sustainable mixtures, J Clean Prod 362 (2022) 132231.

[7]. M.R. Hossain, R. Sultana, M.M. Patwary, N. Khunga, P. Sharma, S.J. Shaker, Self-healing concrete for sustainable buildings. A review, Environ Chem Lett 20(2) (2022) 1265-1273.

[8]. Z. Cao, L. Shen, J. Zhao, L. Liu, S. Zhong, Y. Sun, Y. Yang, Toward a better practice for estimating the CO2 emission factors of cement production: An experience from China, J Clean Prod 139 (2016) 527-539.

[9]. M. Zajac, L. Irbe, F. Bullerjahn, H. Hilbig, M. Ben Haha, Mechanisms of carbonation hydration hardening in Portland cements, Cement Concrete Res 152 (2022) 106687.

[10]. N. Zhang, Z. Luo, Y. Liu, W. Feng, N. Zhou, L. Yang. Towards low-carbon cities through building-stock-level carbon emission analysis: a calculating and mapping method, Sustain Cities Soc 78 (2022) 103633.

[11]. G. Churkina, A. Organschi, C.P.O. Reyer, A. Ruff, K. Vinke, Z. Liu, B.K. Reck, T.E. Graedel, H.J. Schellnhuber, Buildings as a global carbon sink, Nat Sustain 3(4) (2020) 269-276.
[12]. T. Ramesh, R. Prakash, K.K. Shukla, Life cycle energy analysis of buildings: An overview, Energ Buildings 42(10) (2010) 1592-1600.
[13]. S.X. Zhang, Y.L. Sun, Research on life cycle carbon balance of concrete structure buildings, Ecological Economy 05(31) (2015) 78-82.
[14]. F. Xi, S.J. Davis, P. Ciais, D. Crawford-Brown, D. Guan, C. Pade, T. Shi, M. Syddall, J. Lv, L. Ji, L. Bing, J. Wang, W. Wei, K. Yang, B. Lagerblad, I. Galan, C. Andrade, Y. Zhang, Z. Liu, Substantial global carbon uptake by cement carbonation, Nat Geosci 9(12) (2016) 880-883.
[15]. J.W.L.B. Zi Huang, L.N.D.T. Mingjing Ma, A.Z.L. Fengming Xi, Global carbon uptake of cement carbonation
   a. accounts 1930–2021, Earth Syst Sci Data 15 (2023) 4947-4958.
[16]. R. Andersson, K. Fridh, H. Stripple, M. Haglund, Calculating CO2 uptake for existing concrete structures during and after service life, Environ Sci Technol 47(20) (2013) 11625-33.
[17]. L.I. Pei-ying, S. Tie-mao, W. Zi-tong, Measurement method and model of carbon sink from monomer to regional building, Architecture Technology 50(6) (2019) 714-718.
[18]. K. Yang, E. Seo, S. Tae, Carbonation and CO2 uptake of concrete, Environ Impact Asses 46 (2014) 43-52.
[19]. P. Li, T. Shi, L. Bing, Z. Wang, F. Xi, Calculation method and model of carbon sequestration by urban buildings: An example from Shenyang, J Clean Prod 317 (2021) 128450.
[20]. R. Zhao, X. Huang, J. Xue, X. Guan, A practical simulation of carbon sink calculation for urban buildings: A case study of Zhengzhou in China, Sustain Cities Soc 99 (2023) 104980.
[21]. P. Liu, Z. Yu, Y. Chen, Carbonation depth model and carbonated acceleration rate of concrete under different environment, Cement and Concrete Composites 114 (2020) 103736.
[22]. D.S.T.J. Cheng, J.T.J.J. Guo, Chengdu Statistical Yearbook, China Statistics Press2023.
[23]. D. Zhuowen, Z. Qingqing, L.I. Honggang, Extracting Height Information of Urban Buildings Using High-resolution Aerial Image Shadows, Science & Technology Information 18(23) (2020) 47-51.
[24]. Z.R. Jiang, Building Construction Calculation Manual, China Architecture & Building Press2018.
[25]. H.R.M.G. Zhong, Specification for mix proportion design of ordinary concrete, China Architecture & Building Press, 2011.
[26]. H.R.M.G. Zhong, Design code for residential buildings, China Architecture & Building Press, 2011.
[27]. G.J.X.G. Zhong, Code for design of machinery building architecture, Beijing China Planning Publishing House, 2011.
[28]. H.R.M.G. Zhong, Standard for design of office building, China Architecture & Building Press, 2019.
[29]. .R.M.G. Zhong, H.R.M.G. Zhong, General code for fire protection of buildings
   a. and constructions, Beijing China Planning Publishing House, 2022.
[30]. H.R.M.G. Zhong, China Statistical Yearbook, China Statistics Press1999.
[31]. H. Zhang, D. Ba, Z. Wang, A model for forecasting carbonization depth of concrete, Engineering Journal of Wuhan University 39(5) (2006) 42-45.
[32]. S. Tiemao, Z. Shiwen, L.I. Sui, F.U. Shilei, X.U. Dongxu, A computational method for the carbon sequestration capability of building concrete in the whole life cycle, Journal of Shenyang Jianzhu University Natural Science 31(5) (2015) 829-837.
[33]. L.I. Pei-ying, S. Tie-mao, W. Zi-tong, G. Jian, Research on prediction model of carbon sequestration of concrete building based on carbonization mechanism, Architecture Technology 51(3) (2020) 351-353.
[34]. IPCC, 2006 IPCC guidelines for national greenhouse gas inventories., Institute for Global Environmental Strategies2006.
[35]. C. Andrade, Evaluation of the degree of carbonation of concretes in three environments, Construction Build Materials 230 (2020) 116804.
[36]. C. Pade, M. Guimaraes, The CO2 uptake of concrete in a 100 year perspective, Cement Concrete Res 37(9) (2007) 1348-1356.

[37]. I. Monteiro, F.A. Branco, J.D. Brito, R. Neves, Statistical analysis of the carbonation coefficient in open air concrete structures, Construction Build Materials 29 (2012) 263-269.
[38]. F.M. Xi, J.Y. Wang, T.M. Shi, L.F. Bing, Z. Liu, Cement carbon sink and its contributions to global missing carbon sink, Science Press2018.
[39]. W. Dianchao, X. Jianzhuang, X. Bing, Y. Ji, Carbonation Modification of Recycled Aggregate and Carbon Dioxide Sequestration Analysis, Journal of Tongji University(Natural Science) 50(11) (2022) 1610-1619.
[40]. D. Li, B. Chen, H. Sun, S.A. Memon, X. Deng, Y. Wang, F. Xing, Evaluating the effect of external and internal factors on carbonation of existing concrete building structures, Construction & Building Materials 167 (2018) 73-81.
[41]. A. Silva, R. Neves, J. de Brito, Statistical modelling of carbonation in reinforced concrete, Cement and Concrete Composites 50 (2014) 73-81.
[42]. G. Li, C. Guo, X. Gao, Y. Ji, O. Geng, Time dependence of carbonation resistance of concrete with organic film coatings, Construction & Building Materials 114 (2016) 269-275.
[43]. J. Lv, Z. Cao, X. Hu, Effect of biological coating (Crassostrea gigas) on marine concrete: Enhanced durability and mechanisms, Construction Build Materials 285 (2021) 122914.